Sensors & Actuators: B. Chemical 282 (2019) 339–346

Contents lists available at ScienceDirect

Sensors and Actuators B: Chemical

journal homepage: www.elsevier.com/locate/snb

Highly efficient ethanol gas sensor based on hierarchical SnO_2/Zn_2SnO_4 porous spheres

Xueli Yang, Hao Li, Tai Li, Zezheng Li, Weifeng Wu, Chaoge Zhou, Peng Sun*, Fangmeng Liu, Xu Yan, Yuan Gao, Xishuang Liang, Geyu Lu*

State Key Laboratory on Integrated Optoelectronics, Key Laboratory of Gas Sensors, College of Electronic Science and Engineering, Jilin University, 2699 Qianjin Street, Changchun, Jilin Province, 130012, China

ARTICLE INFO

Keywords:
SnO_2/Zn_2SnO_4
Hydrothermal method
Porous sphere
Gas sensor
Ethanol

ABSTRACT

In this work, hierarchucal porous SnO_2/Zn_2SnO_4 nanospheres were succesfully prepared via a facile one-step hydrothermal method with subsequent calcination process. Scanning electron microscopy (SEM), and transmission electron microscopy (TEM) were employed in order to investigate the structural and morphological properties of the as-prepared composites. The results showed that the SnO_2/Zn_2SnO_4 composites were cpmposed of many porous nanospheres with a uniform diameter of about 500 nm. Moreover, the as-prepared products were used as sensing material for the fabrication of gas sensor. The sensing performance of the sensor was systematically evaluated, and the sensor exhibited excellent ethanol-sensing property. The optimum operating temperature was 250 °C with a reponse of 30.5 toward 100 ppm ethanol. Also, the sensor showed good selectivity, stability and a low detection limit of 0.5 ppm (response 1.4). The good sensing performance of SnO_2/Zn_2SnO_4 nanospheres can be attibuted to the porous structure as well as the heterojunction formed between SnO_2 and $ZnSn_2O_4$.

1. Introduction

During the last decades, gas sensors based on semiconductor metal oxides have attracted extensive attention in the application of air-quality detection, environmental protection, inflammable gas monitoring, human health, and public safety, etc [1–5]. Semiconductor metal oxides due to their merits of easy fabrication, low cost and energy consumption, small in size and good chemical stability have received much scientific attention and regarded as important promising materials for gas sensors. Up to now, many semiconductor metal oxides such as ZnO [6–8], α-Fe_2O_3 [9–11], In_2O_3 [12–14], SnO_2 [15–17], WO_3 [18–20] and NiO [21–23] have been successfully developed and used as gas sensing materials, some achivements have been obtained. However, the design and fabrication of new type sensing material for ever increasing the selectivity, sensitivity and decreasing the detection limit still remains a scientific challenge.

In the last decades, some complex oxides have attracted widely interest with the possibility to optimize physical and chemical properties of gas sensors. Some complex oxides including ZnO/SnO_2 [24–26], $ZnO/\alpha\text{-}Fe_2O_3$ [27,28], $\alpha\text{-}Fe_2O_3/NiO$ [29–31], In_2O_3/SnO_2 [32,33] and CuO/SnO_2 [34–36], etc. have been already reported as gas sensing materials. Compared with single oxides sensing materials, complex oxides usually have higher sensitivity, better stabily and lower detection limit. However, novel sensing materials with special structure is still needed to study in order to aquire high performance gas sensor. Spinel oxides with a formula of AB_2O_4 are very promising complex oxides for gas sensing application [37–41]. Zinc stannate (Zn_2SnO_4) is an important ternary oxide with an inverse spinel structure and have a band gap of 3.6 eV [42]. Due to its high chemical sensitivity, low visible absorption and excellent optical electronic properties Zn_2SnO_4 is a proming functional material in various advanced technologies, such as solar cells [43–45], photocatalyst [46], lithium ion battery [47] and gas sensors [48–50]. It is well kown that the gas sensing characteristics are highly dependent on its morpholoy, composition and structure such as porosity, grain size and surface area [51–53]. To date, many nanostructured Zn_2SnO_4 with different morphologies and structures including nanowires, nanorods, nanospheres and polyhedrons were reported to detect volatile organic gases (VOCs) [49,50,54–57]. However, as far as we know, controlled synthesis of porous SnO_2/Zn_2SnO_4 nanospheres with excellent sensing properties toward ethanol has been rarely reported.

In this work, hierachical porous SnO_2/Zn_2SnO_4 nanospheres were

* Corresponding authors.
E-mail addresses: pengsun@jlu.edu.cn (P. Sun), lugy@jlu.edu.cn (G. Lu).

https://doi.org/10.1016/j.snb.2018.11.070
Received 14 July 2018; Received in revised form 30 October 2018; Accepted 13 November 2018
Available online 15 November 2018

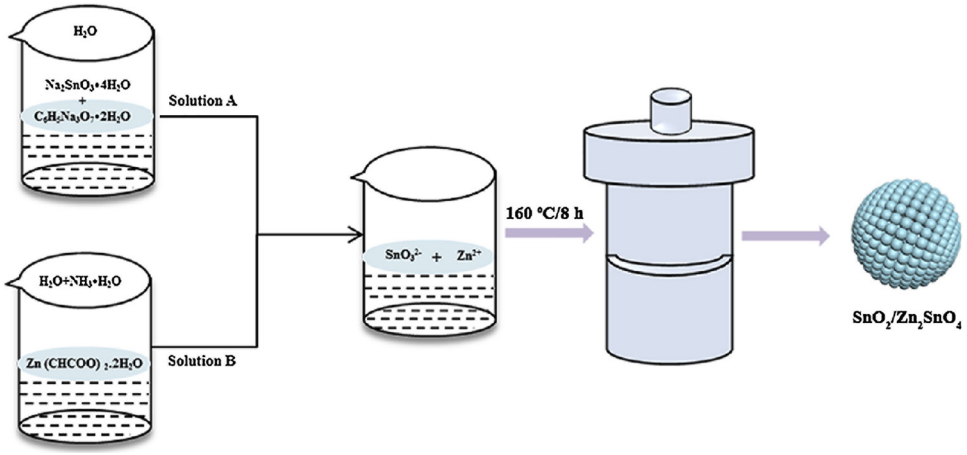

Fig. 1. Schematic diagram of the experimental procedure.

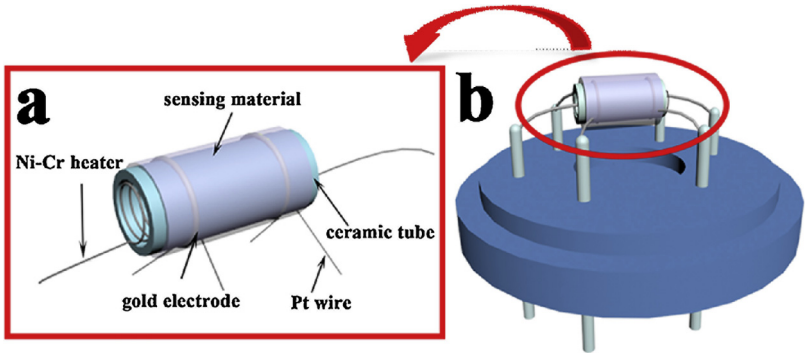

Fig. 2. (a and b) Schematic diagram of the sensor device.

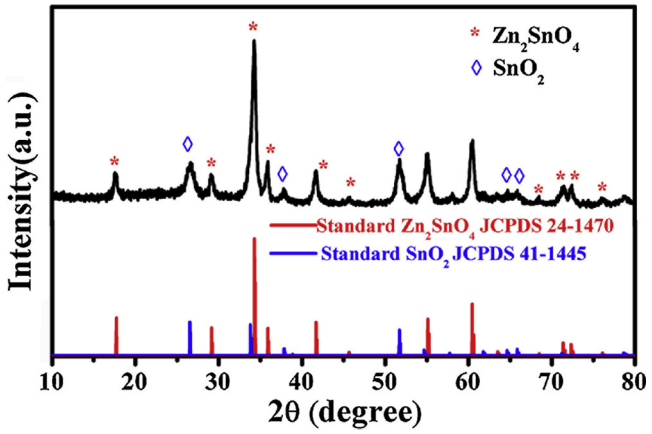

Fig. 3. XRD pattern of SnO_2/Zn_2SnO_4 porous sphere.

successfully prepared via a one-step hydrothermal process. The morphology, microstructure and crystallization properties were conducted by XRD, SEM and TEM techniques. The as-prepared pruducts were fabricated as gas sensor and the gas sensing properties were systematically studied. Compared with SnO_2/Zn_2SnO_4, Zn_2SnO_4 and SnO_2 nanoparticles the as-prepared porous SnO_2/Zn_2SnO_4 nanospheres exhibited excellent gas sensing properties toward ethanol. At the optimum operating temperature of 250 °C, the sensor based on porous SnO_2/Zn_2SnO_4 nanospheres have the highest response of 30.5–100 ppm ethanol. The gas sensing machemism was also discussed in detail.

2. Experimental

2.1. Synthesis process

All reagents used in the experiments were of analytical grade and directly used without any further purification.

The SnO_2/Zn_2SnO_4 composites were synthesized through a facile hydrothermal method. In a typical procedure: 0.284 g of $Na_2SnO_3{\cdot}4H_2O$ and 0.02 g of trisodium citrate dihydrate ($C_6H_5Na_3O_7{\cdot}2H_2O$) were dissoved in 10 mL of deionized water (named as solution A), and then 0.438 g of Zn (CHCOO) $_2{\cdot}2H_2O$ was dissolved in a mixture of 2 mL of deionized water and 5 mL of ammonia hydroxide (named as solution B). After stirred for a while, solution A was mixed with solution B and then stirred for another 15 min at room temperature. Then the mixed solution was transffered into a 50 mL of Teflon-lined autoclave and kept at 160 °C for 8 h. After the completion of reaction, the autoclave was allowed to cool down to room temperature. The whilte precipitates were collected by centrifugation, washed with deionized water and absolute ethanol alternately for several times and dried in air at 80 °C for about 10 h. Finally, the precipitate was annealed at 800 °C for 0.5 h in air atmosphere with a heating rate of 5 °C min^{-1}, and the porous SnO_2/Zn_2SnO_4 composites were obtained. The synthesis process was displayed in Fig. 1. The synthesis procedure of SnO_2/Zn_2SnO_4, Zn_2SnO_4 and SnO_2 nanoparticles were described in the supporting information.

2.2. Characterization

The crystal structure of the as-prepared products was examined by X-ray powder diffraction (XRD) on a Rigaku D/Max-2550 V diffractometer using Cu-Kα radiation (λ = 1.54178 Å). The morphologies and crystal structures of the as-prepared sample were observed by field

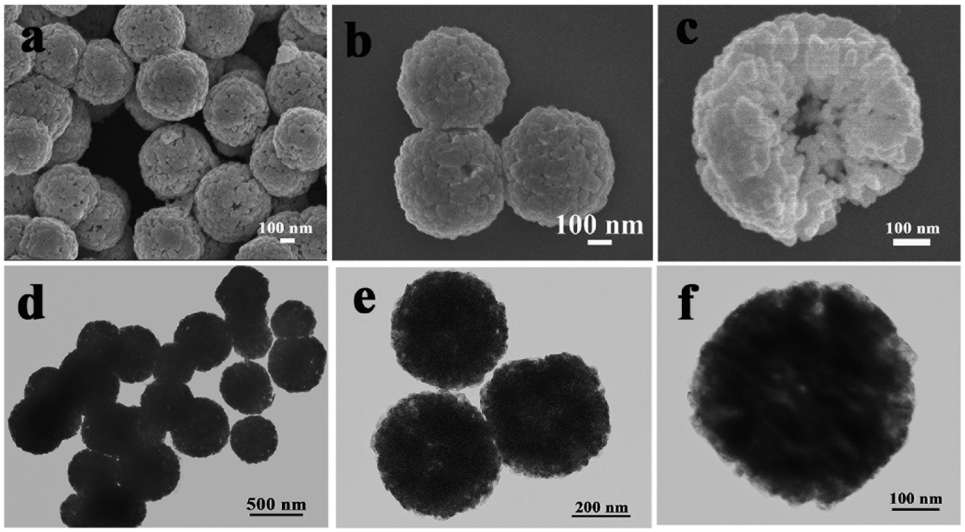

Fig. 4. (a–c) SEM and (d–f) TEM images of the as-prepared SnO_2/Zn_2SnO_4 porous spheres.

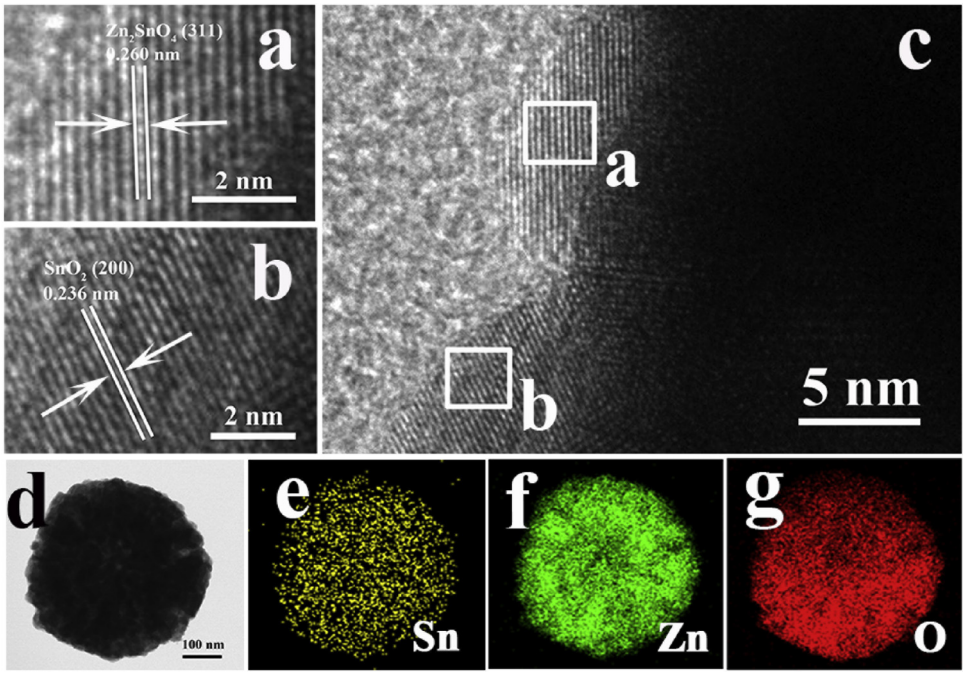

Fig. 5. (a–c) HRTEM images of the as-prepared SnO_2/Zn_2SnO_4 porous spheres. (d–g) TEM images of an individual microsphere and the corresponding elemental mapping images.

emission scanning electron microscopy (FESEM) on a JSM-7500 F (JEOL) microscope operating at an accelerating voltage of 15 kV. Transmission electron microscopy (TEM) and high-resolution transmission electron microscopy (HRTEM) observations were carried out on a JEM-2200FS apparatus (JEOL) operating at 200 kV. Elemental mapping imsges was explored by TEM attachment.

2.3. Fabrication and measurement of gas sensor

The fabrication process of the gas sensor devices could be described as follows: first, the as-obtained products were mixed with an appropriate amount of deionized water to form a homogeneous slurry, and then the slurry was coated on the surface of an alumina tube with the help of a small brush to form a thick film. The alumina tube is 4 mm in length, 1.2 mm in external diameter, and 0.8 mm in internal diameter, the tube was attached with a pair of gold electrodes and each electrode was connected with a pair of Pt wires. After drying in air at room temperature, the device was then calcined at 400 °C for 2 h to enhance the stability of the gas sensors. Afterwards, a Ni-Cr alloy coil was inserted into the alumina tube as a heater to control the operating temperature of the sensor by adjusting the heating current. Then the device was welded on a socket. The schematic diagram of such device was shown in Fig. 2a and b. The gas-sensing performance of the sensor was evaluated under laboratory conditions (30 RH%, 23 °C). The measurement was processed by a static process: a given amount of the tested gas was injected into a closed glass chamber, and the sensor was put into the chamber for the measurement of the sensing performance. The response of the sensor is defined as R_a/R_g, where R_a and R_g are the resistance of the sensor in air and in target gas. The definition of response and recovery times is the time taken by the sensor to achieve 90% of the total resistance change in the case of adsorption and desorption of the tested gases [29].

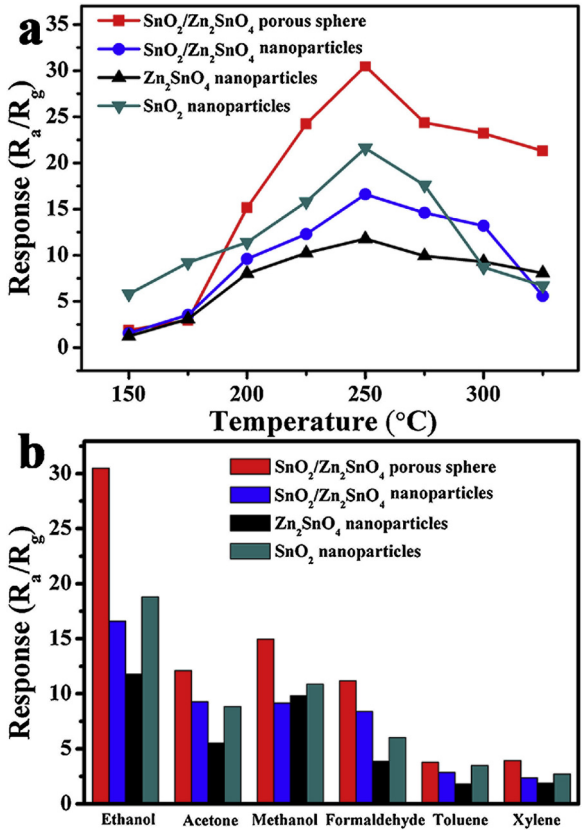

Fig. 6. (a) Response of SnO_2/Zn_2SnO_4 porous spheres, SnO_2/Zn_2SnO_4, Zn_2SnO_4 and SnO_2 nanoparticles at different working temperature upon exposure to 100 ppm ethanol, (b) Response of the four sensors to various test gases with a concentration of 100 ppm.

3. Results and discussion

3.1. Structural and morphological characterization

The phase compositions of the as-prepared SnO_2/Zn_2SnO_4 samples were identified by X-ray powder diffraction (XRD). As shown in Fig. 3, most of the diffraction peaks can be assigned to spinel Zn_2SnO_4 and the rest peaks to SnO_2, which indicates that the as-prepared products was a composite of Zn_2SnO_4 and SnO_2. Moreover, Zn_2SnO_4 and SnO_2 in the composite were in good agreement with the inverse spinel Zn_2SnO_4 (JCPDS: 74–2184) and tetragonal SnO_2 (JCPDS: 41–1445). And no other peaks could be found in the XRD patterns of SnO_2/Zn_2SnO_4 composite, which indicated that the SnO_2/Zn_2SnO_4 composites were of high purity.

Fig. 4a-c is the typical SEM morphology of the SnO_2/Zn_2SnO_4 composites. The as-prepared composites were of well-dispersed with a sphere-like morphology, and the diameter of the composites was about 500 nm. Moreover, from the high-magnification SEM image of Fig. 4c, the as-obtained SnO_2/Zn_2SnO_4 spheres were composed of many nanoparticles and forming a hierarchical structure. TEM measurement was applied to get further information of the structure. As depict in Fig. 4d–f, it is evident that the TEM images showed spherical morphology which was in good accordance with the SEM observations. The SnO_2/Zn_2SnO_4 spheres were uniformly dispersed with a diameter of about 500 nm. Furthermore, in the high-magnified TEM image of Fig. 4f, there are bright spots existed, indicating a porous micro-structure of the as-prepared SnO_2/Zn_2SnO_4 composites. The SEM images of SnO_2/Zn_2SnO_4, pure SnO_2 and Zn_2SnO_4 nanoparticles were displayed in Fig. S2.

HRTEM observation was further performed to confirm the morphogical and crystalline structure of the SnO_2/Zn_2SnO_4 spheres. Fig. 5a and b displays the high-resolution TEM (HRTEM) images obtained from the marked white rectangles in Fig. 5c. In Fig. 5a and b, the lattice fringes could be clearly observed and the spacing of adjacent lattice fringes were measured to be 0.260 and 0.236 nm, which were corresponded to (311) and (200) lattice plane of SnO_2 and Zn_2SnO_4, respectively. In addition, TEM elemental mapping is conducted to confirmm the spatial distribution of Sn, Zn, and O in the spherical structure of Fig. 5d. As shown in Fig. 5e-g, it can be found that Sn, Zn, and O were homogeneously co-existed in the hierachical structure.

3.2. Gas sensing properties

Since operating temperature plays an important role on the semiconductor metal oxide based gas sensors, the respones of the sensors based on SnO_2/Zn_2SnO_4 porous spheres, SnO_2/Zn_2SnO_4, Zn_2SnO_4 and SnO_2 nanoparticles to 100 ppm ethanol as a function of operating temperature were measured, as displayed in Fig. 6a. As the operating temperature changed from 150 to 350 °C, the responses first increase and then reach the maximum value, afterwards the responses decreased with futher increasing temperature. The optimal operating temperature

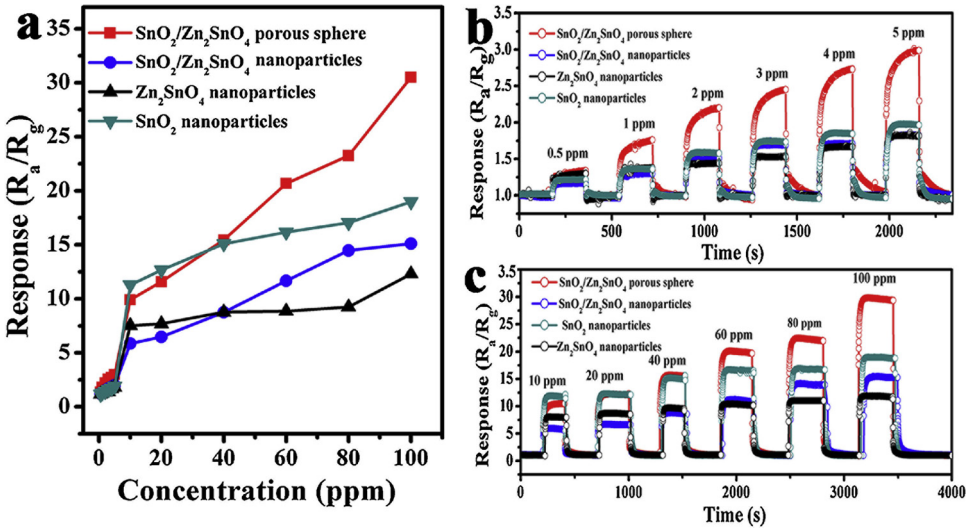

Fig. 7. (a) Response of the four sensors to ethanol with different concentrations at 250 °C. (b and c) Corresponding dynamic response curves of the four sensors to different concentrations of ethanol.

Table 1
Comparison of ethanol sensing performance of gas sensors based on other material in previous reports.

Sensing material	Morphology	Ethanol Con. (ppm)	Tem. (°C)	Res. (R_a/R_g)	Ref.
Zn_2SnO_4/SnO_2	Octahedral-like	100	200	14	[48]
Zn_2SnO_4	Flower-like	100	380	30.8	[57]
Zn_2SnO_4	Nanowires	50	500	21.6	[58]
SnO_2-ZnO	Nanostructures	100	400	16	[59]
SnO_2	Nanorods	50	300	12.4	[60]
SnO_2	Hollow sphere	500	350	23.5	[61]
SnO_2/Zn_2SnO_4	Porous spheres	100	250	30.5	This work

for the four gas sensors was 250 °C with responses of 30.5 (SnO_2/Zn_2SnO_4 porous spheres), 16.6 (SnO_2/Zn_2SnO_4 nanoparticle), 11.7 (Zn_2SnO_4 nanoparticle), and 21.6 (SnO_2 nanoparticle), respectively. Obviously, the sensor based on SnO_2/Zn_2SnO_4 porous spheres exhibited the highest gas response toward ethanol, and then SnO_2 nanoparticles. It is worth noting that after grinded the SnO_2/Zn_2SnO_4 nanoparticles exhibited only half of the response value as compared to SnO_2/Zn_2SnO_4 porous spheres.

Selectivity is an important parameter of gas sensors, the selectivity of the sensor based on SnO_2/Zn_2SnO_4 porous spheres, SnO_2/Zn_2SnO_4, Zn_2SnO_4 and SnO_2 nanoparticles were investigated as shown in Fig. 6b. The bar graph of the four sensors toward various kinds of volatile organic gases, including ethanol, acetone, methanol, formaldehyde, toluene and xylene with a concentration of 100 ppm at their optimum operating temperature of 250 °C was listed. Clearly, it can be seen that all of the four sensors displayed the highest gas response toward ethanol, and a relatively lower response to the other tested gases. In addition, it is worth noting that for the sensor based on SnO_2/Zn_2SnO_4 porous spheres, the gas response to ethanol, acetone, methanol, formaldehyde, toluene and xylene was 30.5, 12.1, 14.9, 11.2, 3.8, and 3.9, respectively. The gas respponse value toward ethanol was 2–8 times higher than to other tested gases, which indicated that the sensor based on porous SnO_2/Zn_2SnO_4 spheres possesses a high response and good selectivity to ethanol.

Fig. 7a–c is the sensing beaviour of the four sensors when orderly exposed to different concentrations of ethanol at 250 °C. Fig. 7a is the linear curve of the four sensors with the increasing of ethanol concentration, obviously, the four sensors showed nearly a linear increasing with ethanol concentration varied from 0.5 to 5 ppm and 10 to 100 ppm. Fig. 7b and c is the corresponding dynamic response and recovery curves with the ethanol concentration increased from 0.5 to 5 ppm and 10 to 100 ppm. It can be seen that the four senors exhibited a stepwise increase, and the highest response can be observed from the sensor based on porous SnO_2/Zn_2SnO_4 sphere. The corresponding response values were 1.4, 1.7, 2.2, 2.5, 2.7, and 3.0 (Fig.7b) for the ethanol concentration from 0.5 to 5 ppm, and for the concentration from 10 to 100 ppm the response values were 9.9, 11.6, 15.4, 20.6, 23.2, and 30.5 (Fig. 7c). Moreover, the sensor based on porous SnO_2/Zn_2SnO_4 sphere have a low detection limit of 0.5 ppm, which indicates the high sensing property of the sensor. Furthermore, in order to confirm the good sensing characteristic of porous SnO_2/Zn_2SnO_4 spheres based gas sensor, a comparison between porous SnO_2/Zn_2SnO_4 spheres and other similar ethanol sensing material in reported literatures was summarized in Table. 1 [49,58–62]. The results indicate that the ethanol response value of sensor based on porous SnO_2/Zn_2SnO_4 spheres exhibited a relatively higher response and lower working temperature.

Response and recovery characteristic is another parameter of gas

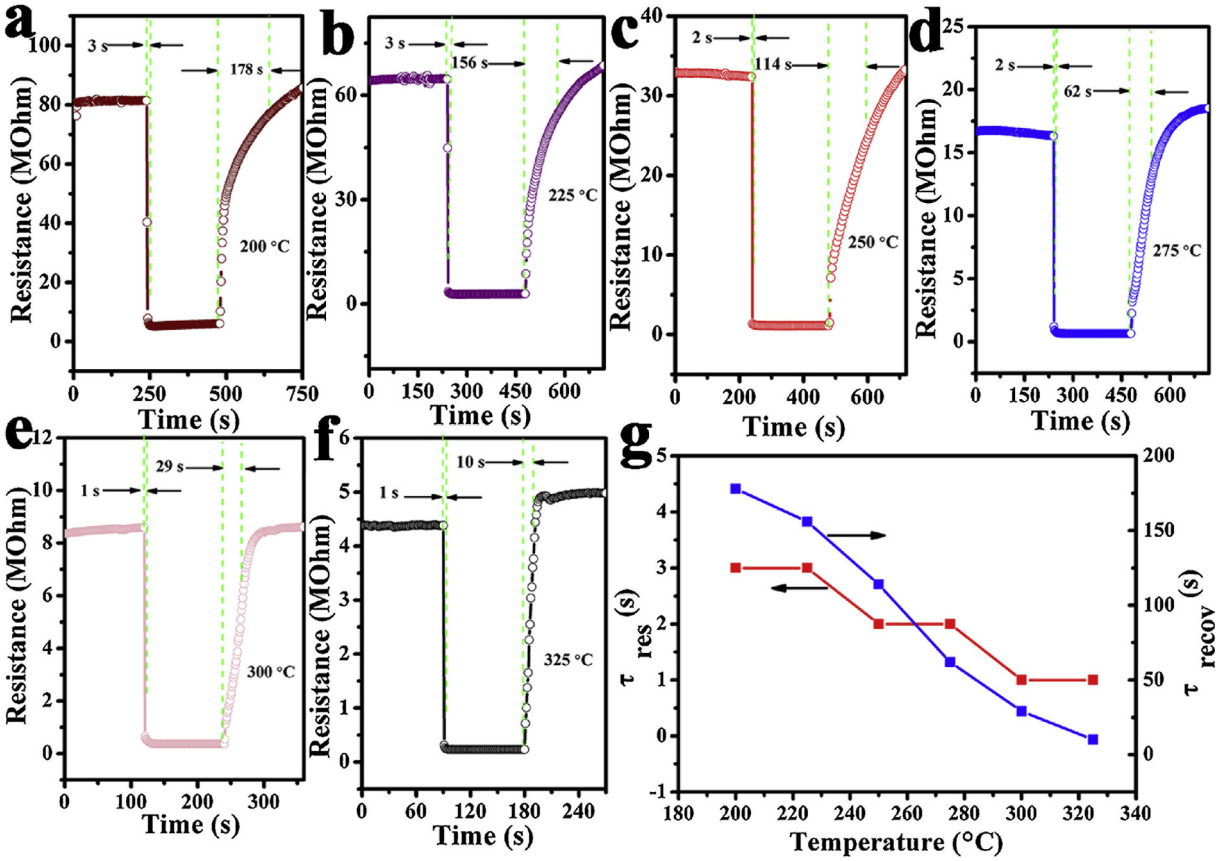

Fig. 8. (a–f) Response transient of the porous SnO_2/Zn_2SnO_4 spheres to 100 ppm ethanol at different working temperature. (g) Response and recovery times of the sensor based on SnO_2/Zn_2SnO_4 spheres at different operating temperature.

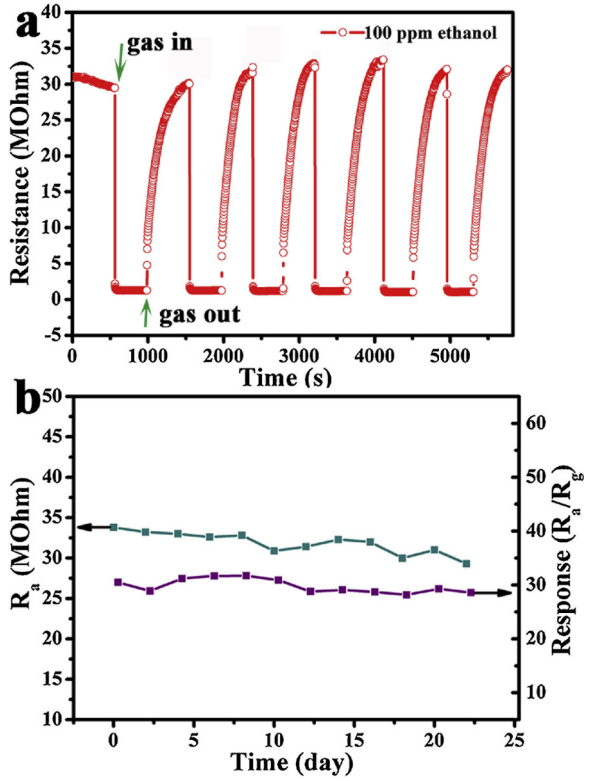

Fig. 9. (a) Six cycles of dynamic response curves of porous SnO_2/Zn_2SnO_4 spheres to 100 ppm ethanol at 250 °C. (b) Resistance in air and responses to 100 ppm ethanol of SnO_2/Zn_2SnO_4 spheres as a function of the test days at 250 °C.

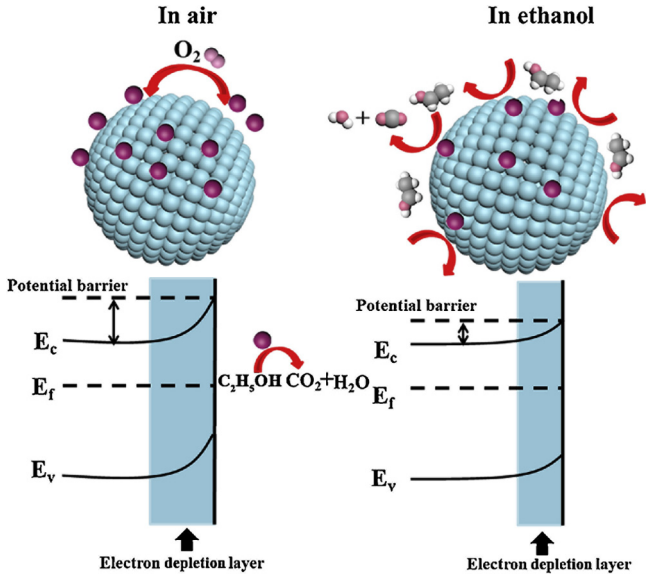

Fig. 10. The schematic illustration of ethanol gas sensing mechanism of porous SnO_2/Zn_2SnO_4 spheres.

sensor. The response and recovery properties of the sensor based on porous SnO_2/Zn_2SnO_4 spheres toward 100 ppm ethanol at different operating temperature were investigated as displayed in Fig. 8a–f. It can be seen that the resistance of the sensor was distinctly decreased with the operating temperature increased from 200 to 325 °C, in addition, the response and recovery time was also varied at different temperature. At the optimum operating temperature of 250 °C, the responsed time was 2 s, and the recovery time was 114 s, respectively. Fig. 7g is the response and recovery time at different operating temperature, the response and recovery time was greatly decreased with increasing operating temperature, and the sensor exhibited a good response and recovery characteristic at the optimal temperature of 250 °C.

As far as we know the reversibility and long-term stability are also important parameters to evaluate gas sensors. Fig. 9a illustrates 6 cycles of response and recovery curve of porous SnO_2/Zn_2SnO_4 sensor to 100 ppm ethanol at 250 °C. The response and recovery curve could be well repeated with similar shape of dynamic transients, demonstrating a good reversibility of the sensor. To further investigate the long-time stability of porous SnO_2/Zn_2SnO_4 based sensor, the response and the resistance in air of the sensor to 100 ppm ethanol at 250 °C during 20 days was measured. As depicted in Fig. 9 b, there is no obvious fluctuation in the resistance and response values during the test days, illustrating good long-term stability of the sensor.

3.3. Gas sensing mechanism

For n-type semiconductor metal oxide based gas sensors, the most widely accepted gas sensing machenism is based on the resistance change in the process of adsorption and desorption of gas molecules and chemical reactions on the surface of sensing materials [53,63,64]. As illustrated in Fig. 10, when the sensor is exposed in ambient air, oxygen molecules will adsorb on the surface of porous SnO_2/Zn_2SnO_4 spheres and ionize to negatively charged surface-adsorbed oxygen species by capturing free electrons from the conducting band of SnO_2/Zn_2SnO_4 composites, as shown in Eqs. (1)—(3):

$$O_{2(gas)} \rightarrow O_{2\ (ads)} \quad (1)$$

$$O_{2(ads)} + e^- \rightarrow O^{2-}{}_{(ads)} \quad (2)$$

$$O^{2-}_{(ads)} + e^- \rightarrow 2O^-{}_{(ads)} \quad (3)$$

As a result, a thick electron depletion layer will form on the sueface of SnO_2/Zn_2SnO_4 spheres, and a high potential barrier is formed between the adjacent nanograins, leading to an increase of resistance in the sensing material. When the sensor is exposed to reducing gas such as ethanol at a moderate temperature, the ethanol molecules would react with the surface adsorbed oxygen species and the captured electrons will release back to the conduction band, resulting in an increasing conductivity and a deceasing resisitance of the sensor. The reaction process between surface adsorbed oxygen species and ethanol is described as Eq. (4):

$$C_2H_5OH + 6O^- \rightarrow 2CO_2 + 3H_2O + 6e- \quad (4)$$

The excellent gas sensing properties of porous SnO_2/Zn_2SnO_4 spheres are mainly attributed to the porous hierarchical structure and the heterojunctions formed between SnO_2 and Zn_2SnO_4. Firstly, compared with SnO_2/Zn_2SnO_4, Zn_2SnO_4 and SnO_2 nanoparticles, the hierarchical SnO_2/Zn_2SnO_4 spheres with porous microstructure could provide a higher accessible surface (as shown in Fig. S3 and Table. S1), and beneficial to gas diffusion and adsorption. Therefore, more surface active sites are available for the reaction between adsorbed oxygen and tested gases, leading to an increasing utilization of the sensing body. While for SnO_2/Zn_2SnO_4 nanoparticles the porous hierarchical architecture was destroyed, the oxygen and target gas could only adsorb on the surface of the material, resulting in a low utilization of the sensing body and a relatively low gas response. Another reason is the heterojunction formed between Zn_2SnO_4 and SnO_2. Accoding to the literature, heterojunctions formed between different semiconductor oxides could make a significant contribution to the gas sensing performance [50,65,66]. Due to the different band gap energy and work function of Zn_2SnO_4 and SnO_2, electrons will be transffered between the two semiconductor oxides, forming heterojunctions at the SnO_2/Zn_2SnO_4 interfaces. As the conduction band edge of Zn_2SnO_4 locates at higher

potential than SnO_2, the electrons in the conduction band of Zn_2SnO_4 would migrate to the conduction band of SnO_2 until their Femi level become euqal [67,68]. This process will result in the generation of additional electron depletion in the interface of SnO_2/Zn_2SnO_4 composites, which will play an important role in the sensing reactions, and resulting in an enhanced sensing performance.

4. Conclusions

In summary, we have successfully prepared hierarchical porous SnO_2/ Zn_2SnO_4 spheres via a one-step hydrothermal method with subsequent calcination treatment. The results indicated that the SnO_2/ Zn_2SnO_4 spheres were composed of many SnO_2/ Zn_2SnO_4 nanoparticles forming a hierarchical porous micro-structure. The SnO_2/ Zn_2SnO_4 composites were used as gas sensing material and the gas sensing performances of the as-fabricated gas sensor were systematically investigated. The results indicated that compared with SnO_2/ Zn_2SnO_4, Zn_2SnO_4 and SnO_2 nanoparticles the sensor based on porous SnO_2/ Zn_2SnO_4 composites displayed excellent gas sensing properties toward ethanol, including high gas response, good reversibility and outstanding selectivity. Moreover, the sensor showed a low detection limit of 0.5 ppm with a response value of 1.4. The good sensing performance can be mainly attributed to the unique porous structure and heterojunction formed between SnO_2 and Zn_2SnO_4. This work indicates that porous SnO_2/Zn_2SnO_4 composites are very promising sensing material for the application of ethanol gas sensor.

Acknowledgements

This work is supported by the National Key Research and Development Program (No. 2016YFC0207300). National Nature Science Foundation of China (Nos. 61722305, 61503148, 61520106003, 61327804). Science and Technology Development Program of Jilin Province (No. 20170520162JH). China Postdoctoral Science Foundation funded project Nos. 2017T100208 and 2015M580247. Program for JLU Science and Technology Innovative Research Team. Fundamental Research Funds for the Central Universities.

Appendix A. Supplementary data

Supplementary material related to this article can be found, in the online version, at doi:https://doi.org/10.1016/j.snb.2018.11.070.

References

[1] A. Modi, N. Koratkar, E. Lass, B.Q. Wei, P.M. Ajayan, Miniaturized gas ionization sensors using carbon nanotubes, Nature 424 (2003) 171–174.
[2] B. Timmer, W. Olthuis, A. van den Berg, Ammonia sensors and their applications-a review, Sens. Actuators B Chem. 107 (2005) 666–677.
[3] M. Meyyappan, Carbon nanotube-based chemical sensors, Small 12 (2016) 2118–2129.
[4] J.-W. Yoon, J.-H. Lee, Toward breath analysis on a chip for disease diagnosis using semiconductor-based chemiresistors: recent progress and future perspectives, Lab Chip 17 (2017) 3537–3557.
[5] D.R. Patil, L.A. Patil, Cr_2O_3-modified ZnO thick film resistors as LPG sensors, Talanta 77 (2009) 1409–1414.
[6] H. Nguyen Hai, T. Dao Duc, H. Nguyen Thanh, P. Nguyen Huy, T. Phan Duy, H. Hoang Si, Fast response of carbon monoxide gas sensors using a highly porous network of ZnO nanoparticles decorated on 3D reduced graphene oxide, Appl. Surf. Sci. 434 (2018) 1048–1054.
[7] J.X. Wang, X.W. Sun, Y. Yang, H. Huang, Y.C. Lee, O.K. Tan, L. Vayssieres, Hydrothermally grown oriented ZnO nanorod arrays for gas sensing applications, Nanotechnology 17 (2006) 4995–4998.
[8] J. Zhang, S. Wang, M. Xu, Y. Wang, B. Zhu, S. Zhang, W. Huang, S. Wu, Hierarchically porous ZnO architectures for gas sensor application, Cryst. Growth Des. 9 (2009) 3532–3537.
[9] X. Hu, J.C. Yu, J. Gong, Q. Li, G. Li, Alpha-Fe_2O_3 nanorings prepared by a microwave-assisted hydrothermal process and their sensing properties, Adv. Mater. 19 (2007) 2324–2329.
[10] Y. Wang, Y. Wang, J. Cao, F. Kong, H. Xia, J. Zhang, B. Zhu, S. Wang, S. Wu, Low-temperature H_2S sensors based on Ag-doped alpha-Fe_2O_3 nanoparticles, Sens. Actuators B Chem. 131 (2008) 183–189.
[11] K. Tian, X.-X. Wang, Z.-Y. Yu, H.-Y. Li, X. Guo, Hierarchical and hollow Fe_2O_3 nanoboxes derived from metal-organic frameworks with excellent sensitivity to H_2S, ACS Appl. Mater. Interfaces 9 (2017) 29669–29676.
[12] C. Li, D.H. Zhang, X.L. Liu, S. Han, T. Tang, J. Han, C.W. Zhou, In_2O_3 nanowires as chemical sensors, Appl. Phys. Lett. 82 (2003) 1613–1615.
[13] A. Gurlo, Nanosensors: towards morphological control of gas sensing activity. SnO_2, In_2O3, ZnO and WO3 case studies, Nanoscale 3 (2011) 154–165.
[14] M. Ding, N. Xie, C. Wang, X. Kou, H. Zhang, L. Guo, Y. Sun, X. Chuai, Y. Gao, F. Liu, P. Sun, G. Lu, Enhanced NO_2 gas sensing properties by Ag-doped hollow urchin-like In_2O_3 hierarchical nanostructures, Sens. Actuators B Chem. 252 (2017) 418–427.
[15] N. Barsan, U. Weimar, Understanding the fundamental principles of metal oxide based gas sensors; the example of CO sensing with SnO_2 sensors in the presence of humidity, J. Phys-Condens. Mat. 15 (2003) R813–R839.
[16] E.R. Leite, I.T. Weber, E. Longo, J.A. Varela, A new method to control particle size and particle size distribution of SnO_2 nanoparticles for gas sensor applications, Adv. Mater. 12 (2000) 965–968.
[17] S.-H. Lee, V. Galstyan, A. Ponzoni, I. Gonzalo Juan, R. Riedel, M.-A. Dourges, Y. Nicolas, T. Toupance, Finely tuned SnO_2 nanoparticles for efficient detection of reducing and oxidizing gases: the influence of alkali metal cation on gas sensing properties, ACS Appl. Mater. Interfaces 12 (2018) 10173–10184.
[18] J. Ma, Y. Ren, X. Zhou, L. Liu, Y. Zhu, X. Cheng, P. Xu, X. Li, Y. Deng, D. Zhao, Pt nanoparticles sensitized ordered mesoporous WO_3 semiconductor: gas sensing performance and mechanism study, Adv. Funct. Mater. 28 (2018).
[19] Y. Shen, H. Bi, T. Li, X. Zhong, X. Chen, A. Fan, D. Wei, Low-temperature and highly enhanced NO_2 sensing performance of Au-functionalized WO_3 microspheres with a hierarchical nanostructure, Appl. Surf. Sci. 434 (2018) 922–931.
[20] Y. Shen, W. Wang, X. Chen, B. Zhang, D. Wei, S. Gao, B. Cui, Nitrogen dioxide sensing using tungsten oxide microspheres with hierarchical nanorod-assembled architectures by a complexing surfactant-mediated hydrothermal route, J. Mater. Chem. A Mater. Energy Sustain. 4 (2016) 1345–1352.
[21] B. Liu, H. Yang, H. Zhao, L. An, L. Zhang, R. Shi, L. Wang, L. Bao, Y. Chen, Synthesis and enhanced gas-sensing properties of ultralong NiO nanowires assembled with NiO nanocrystals, Sens. Actuators B Chem. 156 (2011) 251–262.
[22] G. Zhu, C. Xi, H. Xu, D. Zheng, Y. Liu, X. Xu, X. Shen, Hierarchical NiO hollow microspheres assembled from nanosheet-stacked nanoparticles and their application in a gas sensor, RSC Adv. 2 (2012) 4236–4241.
[23] Y. Zhang, W. Zeng, New insight into gas sensing performance of nanoneedle-assembled and nanosheet-assembled hierarchical NiO nanoflowers, Mater. Lett. 195 (2017) 217–219.
[24] S.-W. Choi, J.Y. Park, S.S. Kim, Synthesis of SnO_2-ZnO core-shell nanofibers via a novel two-step process and their gas sensing properties, Nanotechnology 20 (2009) 465603.
[25] S. Park, S. An, Y. Mun, C. Lee, UV-enhanced NO_2 gas sensing properties of SnO_2-core/ZnO-shell nanowires at room temperature, ACS Appl. Mater. Interfaces 5 (2013) 4285–4292.
[26] L. Ma, S.Y. Ma, H. Kang, X.F. Shen, T.T. Wang, X.H. Jiang, Q. Chen, Preparation of Ag-doped ZnO-SnO_2 hollow nanofibers with an enhanced ethanol sensing performance by electrospinning, Mater. Lett. 209 (2017) 188–192.
[27] S. Ghosh, D. Adak, R. Bhattacharyya, N. Mukherjeee, ZnO/gamma-Fe2O_3 charge transfer interface toward highly selective H2S sensing at a low operating temperature of 30 degrees C, ACS Sens. 2 (2017) 1831–1838.
[28] C.L. Zhu, Y.J. Chen, R.X. Wang, L.J. Wang, M.S. Cao, X.L. Shi, Synthesis and enhanced ethanol sensing properties of alpha-Fe_2O_3/ZnO heteronanostructures, Sens. Actuators B Chem. 140 (2009) 185–189.
[29] C. Wang, X. Cheng, X. Zhou, P. Sun, X. Hu, K. Shimanoe, G. Lu, N. Yamazoe, Hierarchical alpha-Fe_2O_3/NiO composites with a hollow structure for a gas sensor, ACS Appl. Mater. Interfaces 6 (2014) 12031–12037.
[30] J. Cao, Z. Wang, R. Wang, S. Liu, T. Fei, L. Wang, T. Zhang, Synthesis of core-shell alpha-Fe_2O_3@NiO nanofibers with hollow structures and their enhanced HCHO sensing properties, J. Mater. Chem. A Mater. Energy Sustain. 3 (2015) 5635–5641.
[31] M. ul Haq, Z. Wen, Z. Zhang, S. Khan, Z. Lou, Z. Ye, L. Zhu, A two-step synthesis of nanosheet-covered fibers based on alpha-Fe_2O_3/NiO composites towards enhanced acetone sensing, Sci. Rep. 8 (2018).
[32] Y. Liu, S. Yao, Q. Yang, P. Sun, Y. Gao, X. Liang, F. Liu, G. Lu, Highly sensitive and humidity-independent ethanol sensors based on In_2O_3 nanoflower/SnO_2 nanoparticle composite, RSC Adv. 5 (2015) 52252–52258.
[33] H. Du, J. Wang, M. Su, P. Yao, Y. Zheng, N. Yu, Formaldehyde gas sensor based on SnO_2/In_2O_3 hetero-nanofibers by a modified double jets electrospinning process, Sens. Actuators B Chem. 166 (2012) 746–752.
[34] A. Chowdhuri, P. Sharma, V. Gupta, K. Sreenivas, K.V. Rao, H_2S gas sensing mechanism of SnO_2 films with ultrathin CuO dotted islands, J. Appl. Phys. 92 (2002) 2172–2180.
[35] A. Katoch, J.-H. Kim, S.S. Kim, Significance of the nanograin size on the H_2S-sensing ability of CuO-SnO_2 composite nanofibers, J. Sensors (2015).
[36] S. Bai, W. Guo, J. Sun, J. Li, Y. Tian, A. Chen, R. Luo, D. Li, Synthesis of SnO_2-CuO heterojunction using electrospinning and application in detecting of CO, Sens. Actuators B Chem. 226 (2016) 96–103.
[37] A. Sutka, K.A. Gross, Spinel ferrite oxide semiconductor gas sensors, Sens. Actuators B Chem. 222 (2016) 95–105.
[38] J. Wu, D. Gao, T. Sun, J. Bi, Y. Zhao, Z. Ning, G. Fan, Z. Xie, Highly selective gas sensing properties of partially inversed spinel zinc ferrite towards H_2S, Sens. Actuators B Chem. 235 (2016) 258–262.
[39] H. Chen, G.-D. Li, M. Fan, Q. Gao, J. Hu, S. Ao, C. Wei, X. Zou, Electrospinning preparation of mesoporous spinel gallate (MGa_2O_4; M = Ni, Cu, Co) nanofibers and

their M(II) ions-dependent gas sensing properties, Sens. Actuators B Chem. 240 (2017) 689–696.
[40] S. Vijayanand, P.A. Joy, H.S. Potdar, D. Patil, P. Patil, Nanostructured spinet $ZnCo_2O_4$ for the detection of LPG, Sens. Actuators B Chem. 152 (2011) 121–129.
[41] H. Fan, S. Xu, X. Cao, D. Liu, Y. Yin, H. Hao, D. Wei, Y. Shen, Ultra-long Zn_2SnO_4-ZnO microwires based gas sensor for hydrogen detection, Appl. Surf. Sci. 400 (2017) 440–445.
[42] Z. Chen, M. Cao, C. Hu, Novel Zn_2SnO_4 hierarchical nanostructures and their gas sensing properties toward ethanol, J. Phys. Chem. C 115 (2011) 5522–5529.
[43] B. Tan, E. Toman, Y. Li, Y. Wu, Zinc stannate (Zn_2SnO_4) dye-sensitized solar cells, J. Am. Chem. Soc. 129 (2007) 4162–4163.
[44] J. Dou, Y. Li, F. Xie, T.J. Chow, M. Wei, Highly efficient triarylene conjugated dyes for dye-sensitized Zn_2SnO_4 solar cells, Sol. Energy 155 (2017) 1–6.
[45] R. Liu, W. Du, Q. Chen, F. Gao, C. Wei, J. Sun, Q. Lu, Fabrication of Zn_2SnO_4/SnO_2 hollow spheres and their application in dye-sensitized solar cells, RSC Adv. 3 (2013) 2893–2896.
[46] T. Yan, H. Liu, M. Sun, X. Wang, M. Li, Q. Yan, W. Xu, B. Du, Efficient photocatalytic degradation of bisphenol A and dye pollutants over $BiOI/Zn_2SnO_4$ heterojunction photocatalyst, RSC Adv. 5 (2015) 10688–10696.
[47] L. Qin, S. Liang, A. Pan, X. Tan, Zn_2SnO_4/carbon nanotubes composite with enhanced electrochemical performance as anode materials for lithium-ion batteries, Mater. Lett. 164 (2016) 44–47.
[48] X. Chu, R. Hu, J. Wang, Y. Dong, W. Zhang, L. Bai, W. Sun, Preparation and gas sensing properties of graphene-Zn_2SnO_4 composite materials, Sens. Actuators B Chem. 251 (2017) 120–126.
[49] S. Shu, M. Wang, Y. Wei, S. Liu, Synthesis of surface layered hierarchical octahedral-like structured Zn_2SnO_4/SnO_2 with excellent sensing properties toward HCHO, Sens. Actuators B Chem. 243 (2017) 1171–1180.
[50] J. Yang, S. Wang, L. Zhang, R. Dong, Z. Zhu, X. Gao, Zn_2SnO_4-doped SnO_2 hollow spheres for phenylamine gas sensor application, Sens. Actuators B Chem. 239 (2017) 857–864.
[51] J.-H. Lee, Gas sensors using hierarchical and hollow oxide nanostructures: overview, Sens. Actuators B Chem. 140 (2009) 319–336.
[52] N. Yamazoe, G. Sakai, K. Shimanoe, Oxide semiconductor gas sensors, Catal. Surv. Asia 7 (2003) 63–75.
[53] C. Wang, L. Yin, L. Zhang, D. Xiang, R. Gao, Metal oxide gas sensors: sensitivity and influencing factors, Sensors 10 (2010) 2088–2106.
[54] B. Wang, Z.Q. Zheng, L.F. Zhu, Y.H. Yang, H.Y. Wu, Self-assembled and Pd decorated Zn_2SnO_4/ZnO wire-sheet shape nano-heterostructures networks hydrogen gas sensors, Sens. Actuators B Chem. 195 (2014) 549–561.
[55] S. Park, S. An, H. Ko, C. Jin, C. Lee, Enhanced NO_2 sensing properties of Zn_2SnO_4-core/ZnO-shell nanorod sensors, Ceram. Int. 39 (2013) 3539–3545.
[56] L. Wang, T. Zhou, R. Zhang, Z. Lou, J. Deng, T. Zhang, Comparison of toluene sensing performances of zinc stannate with different morphology-based gas sensors, Sens. Actuators B Chem. 227 (2016) 448–455.
[57] S. Zhang, G. Sun, Y. Li, B. Zhang, L. Lin, Y. Wang, J. Cao, Z. Zhang, Continuously improved gas-sensing performance of SnO_2/Zn_2SnO_4 porous cubes by structure evolution and further NiO decoration, Sens. Actuators B Chem. 255 (2018) 2936–2943.
[58] C. Chen, G. Li, J. Li, Y. Liu, One-step synthesis of 3D flower-like Zn_2SnO_4 hierarchical nanostructures and their gas sensing properties, Ceram. Int. 41 (2015) 1857–1862.
[59] T. Tharsika, A.S.M.A. Haseeb, S.A. Akbar, M.F.M. Sabri, Y.H. Wong, Gas sensing properties of zinc stannate (Zn_2SnO_4) nanowires prepared by carbon assisted thermal evaporation process, J. Alloys. Compd. 618 (2015) 455–462.
[60] K. Nguyen Duc, T. Do Dang, D. Nguyen Van, H. Nguyen Duc, H. Nguyen Van, Design of SnO_2/ZnO hierarchical nanostructures for enhanced ethanol gas-sensing performance, Sens. Actuators B Chem. 174 (2012) 594–601.
[61] X. Zhou, W. Fu, H. Yang, D. Ma, J. Cao, Y. Leng, J. Guo, Y. Zhang, Y. Sui, W. Zhao, M. Li, Synthesis and ethanol-sensing properties of flowerlike SnO_2 nanorods bundles by poly(ethylene glycol)-assisted hydrothermal process, Mater. Chem. Phys. 124 (2010) 614–618.
[62] B. Wang, L. Sun, Y. Wang, Template-free synthesis of nanosheets-assembled SnO_2 hollow spheres for enhanced ethanol gas sensing, Mater. Lett. 218 (2018) 290–294.
[63] N. Barsan, U. Weimar, Conduction model of metal oxide gas sensors, J. Electroceram. 7 (2001) 143–167.
[64] X. Li, W. Wei, S. Wang, L. Kuai, B. Geng, Single-crystalline alpha-Fe_2O_3 oblique nanoparallelepipeds: high-yield synthesis, growth mechanism and structure enhanced gas-sensing properties, Nanoscale 3 (2011) 718–724.
[65] X. Wang, S. Zhang, M. Shao, J. Huang, X. Deng, P. Hou, X. Xu, Fabrication of ZnO/$ZnFe_2O_4$ hollow nanocages through metal organic frameworks route with enhanced gas sensing properties, Sens. Actuators B Chem. 251 (2017) 27–33.
[66] S. Wang, J. Zhang, J. Yang, X. Gao, H. Zhang, Y. Wang, Z. Zhu, Spinel $ZnFe_2O_4$ nanoparticle-decorated rod-like ZnO nanoheterostructures for enhanced gas sensing performances, RSC Adv. 5 (2015) 10048–10057.
[67] B. Li, E. Guo, C. Wang, L. Yin, Novel Au inlaid Zn_2SnO_4/SnO_2 hollow rounded cubes for dye-sensitized solar cells with enhanced photoelectric conversion performance, J. Mater. Chem. A Mater. Energy Sustain. 4 (2016) 466–477.
[68] B. Li, L. Luo, T. Xiao, X. Hu, L. Lu, J. Wang, Y. Tang, Zn_2SnO_4-SnO_2 heterojunction nanocomposites for dye-sensitized solar cells, J. Alloys. Compd. 509 (2011) 2186–2191.

Xueli Yang received her B. Eng. degree in 2013 and M.S. degree in 2016 from College of Science, Northeast Forestry University in China. Currently she is studying for her Ph.D. degree in College of Electronic Science and Engineering, Jilin University, China. Her research interests focus on the synthesis and characterization of semiconductor oxide functional materials and gas sensors.

Hao Li He is currently working toward the B.Eng. degree in the Electronics Science and Engineering department, Jilin University, and is currently in the third stage.

Tai Li He enrolled in Department of Electronic Science and engineering, Jilin University, and is currently in the third stage.

ZeZheng Li He is majored in Semiconductor-Chemistry,is a junior of the Electronics Science and Engineering department,Jilin University.

Weifeng Wu He is currently working toward the BS EE degree now in department of Electronic Science and Engineering. And his interests include the synthesis of functional materials and their applications in gas sensors,as well as the functional study of wide bandgap semiconductor.

Chaoge Zhou She is studying for her BS EE degree now in department of Electronic Science and Engineering. And she is going to studying for her MS degree in College of Electroic Science and Engineering,Jilin University,China.

Peng Sun received his PhD degree from College of Electronic Science and Engineering, Jilin University, China in 2014. He was appointed the lecturer in Jilin University in the same year. Now, he is engaged in the synthesis and characterization of the semiconducting functional materials and gas sensors.

Fangmeng Liu received his PhD degree in 2017 from College of Electronic Science and Engineering, Jilin University, China. Now he is a lecturer of Jilin University, China. His current research interests include the application of functional materials and development of solid state electrolyte gas sensor and flexible device.

Xu Yan received his M.S. degree in 2013 from Nanjing Agricultural University. He joined the group of Prof. Xingguang Su at Jilin University and received his Ph.D. degree in June 2017. Since then, he did postdoctoral work with Prof. Geyu Lu. Currently, his research interests mainly focus on the development of the functional nanomaterials for chem/bio sensors.

Yuan Gao received her PhD degree from Department of Analytical Chemistry at Jilin University in 2012. Now she is an associate professor in Jilin University, China. Her current research is focus on the preparation and application of graphene and semiconductor oxide, especial in gas sensor and biosensor.

Xishuang Liang received the B. Eng. degree in Department of Electronic Science and Technology in 2004. He received his Doctor's degree in College of Electronic Science and Engineering at Jilin University in 2009. Now he is an associate professor of Jilin University, China. His current research is solid electrolyte gas sensor.

Geyu Lu received the BS degree in electronic sciences in 1985 and the MS degree in 1988 from Jilin University in China and the Dr. Eng. degree in 1998 from Kyushu University in Japan. Now he is a professor of Jilin University, China. His current research interests include the development of chemical sensors and the application of the function materials.